ΠΑΝΕΠΙΣΤΗΜΙΟ ΚΡΗΤΗΣ

ΣΧΟΛΗ ΘΕΤΙΚΩΝ ΕΠΙΣΤΗΜΩΝ

ΤΜΗΜΑ ΕΠΙΣΤΗΜΗΣ ΚΑΙ ΤΕΧΝΟΛΟΓΙΑΣ ΥΛΙΚΩΝ

ΠΤΥΧΙΑΚΗ ΕΡΓΑΣΙΑ ΤΟΥ ΜΑΡΙΟΥ ΑΔΑΜΙΔΗ

ΑΜ:1367

ΤΙΤΛΟΣ:

Synthesis and photochromic properties of composite AgCl-$AgPO_3$ glasses

ΕΠΙΒΛΕΠΩΝ ΚΑΘΗΓΗΤΕΣ:

ΕΜΜΑΝΟΥΗΛ ΣΤΡΑΤΑΚΗΣ, ΒΛΑΣΣΟΠΟΥΛΟΣ ΔΗΜΗΤΡΙΟΣ

ΗΡΑΚΛΕΙΟ 2022

Abstract

We herein present a simple, low-temperature, post-glass melting encapsulation fabrication protocol in which AgCl thin layers are incorporated within silver metaphosphate glass ($AgPO_3$). The selection of $AgPO_3$ glass is mainly based on its relative 'soft' nature (Tg=192^oC) that allows the feasible embedment of the AgCl layer, while being transparent in most of the visible range, and thus suitable for smart photochromic windows applications. The described synthesis procedure allows the controlled positioning of the AgCl layer within the host glass matrix, while the properties of the layer itself could be modified accordingly. Results show a direct dependence of the composite AgCl-$AgPO_3$ glass photochromic response with the morphological features of the encapsulated AgCl layer, i.e. thickness and position. The photochromic response time upon varying UV irradiation dose is also considered. Ongoing work involves efforts on further enhancing the photochromic performance upon exploiting the presence of silver nanoparticles within the glass, as well as, by introducing periodic patterns on the glass surface by means of laser processing.

Keywords: silver chlroride, silver metaphosphate glass, soft glass, post-glass melting incorporation, photochromic optical properties.

1 Introduction

The development of advanced photochromic, as well as, other color-changing materials have produced a great amount of solutions and potential candidates for many applications in the industry. Products such as photochromic sunglasses, coatings, electrochromic shades on airliners and thermochromic windows for energy efficient buildings, among others, prove color-changing devices to be widely applicable and reliable [1-10]. while offering many advantages in terms of internal temperature regulation, energy saving, and protection from

harmful~~l~~ solar light radiation.

In particular, photochromic devices show great interest in applications where power-less protection from the ionizing parts of the solar radiation is required [3,11]. These compounds show fatigueless transition between two distinct states of different coloration, a darkened and a bleached state. The reversibility of these materials depends on the presence of an activating UV light of a wavelength. When the UV exposure is absent, the material returns to its bleached state. In form of a film or a coating, these properties can offer a composite with quasi-active (require energy to shift but can absorb from the environment) alternating transmissivity characteristics, with a variable ability to absorb UV-Vis-IR radiation for each state of coloration [12].

Silver chloride (AgCl) salt, as a compound among the photochromic class of silver halides, exhibits a reversible alteration in transparency and colour when exposed to sunlight and in particular, under intense ultraviolet (UV) radiation [13,14]. Based on this, it poses an excellent candidate for the development of advanced photochromic materials targeting a variety of applications, such as photochromic lenses [15] and photochromic paper. Aerospace applications in low earth orbit devices is, among others, a typical example in which the remarkable photochromic switching features of the AgCl salt could be exploited. In principle, AgCl crystal can reversibly become non-transparent to the sunlight's harmful ionizing rays that radiate onto the structure and electronics, while being transparent to higher-wavelength light (IR) that induces useful solar heat flux [16]. Despite these benefits, a continuous scientific and technological challenge remains how to design, fabricate and practically employ AgCl coatings and exploit its reversible photochromic features [13,14,17].

On this basis, photochromic glasses are of particular interest due to their transparent look and convenient nature in application. Most commonly with silver chloride, and other photochromic substances, the photochromic crystals of the salt are incorporated inside within

a silica or borosilicate glass matrix during their glass formation. Although silica based glass produces an inexpensive substrate material with excellent transparency, their high glass transition temperatures (Tg) of over 525°C (borosilicate) and 1200°C (silica) is of its own a challenging and costly aspect of the composite fabrication. These high glass transition temperature glasses based on silica, as well as other substrates that need high temperatures to allow encapsulation of films or crystals, fundamentally require large amounts of energy for the wide area panels that need treatment. In addition to the above, devices such as titanium dioxide - tungsten trioxide silica composites [2], alumina - calcium oxide glasses [4] etc., either need high amounts of energy to darken, or heat and prolonged durations to revert.

On a rather different manner, in this work, we propose a simple, low-temperature, non-toxic, self-resorbable, post-glass melting encapsulation fabrication protocol in which AgCl thin layers are incorporated within silver metaphosphate glass $AgPO_3$. The selection of $AgPO_3$ glass is prompted by several reasons, such as enabling a non-toxic, self resorbable encapsulation procedure for the integration of a film such as the photochromic AgCl compound within its highly transparent glass matrix [18-20,24]. The $AgPO_3$ glass has a very low glass transition temperature (Tg=192°C) compared to the silica-based compounds [18]. This is crucial, as it disproportionately lowers the energy required for the incorporation of the film, especially in larger surface areas.

Due to the soft nature of the $AgPO_3$ substrate, the AgCl can be easily integrated with an aquatic solution of AgCl-NH_3 that will be depositioned onto the substrate, and quenched when close to its glass transition temperature. Raman spectroscopy was performed to investigate the effect that the incorporation of the AgCl has on the glass matrix structure [21]. Remarkably, the developed composite AgCl-$AgPO_3$ glasses exhibit reversible photochromic switching upon exposure to UV light with superior response times between the fully transparent and opaque states. Thus, the metaphosphate glass matrix is an excellent candidate to support

fatigueless transition between the states of the AgCl [19]. The developed composite photochromic glasses exhibit interesting photochromic features, with enhanced response times when compared to previously reported similar architectures [2-4,13,14,17,19].

2 Experimental procedures

2.1 Composite glass synthesis

A Pt crucible was employed in this process to synthesize the $AgPO_3$ glass substrate. The starting materials used were dry $NH_4H_2PO_4$ (99.995%) and $AgNO_3$ (99.995%). After weighting, the prepared batches were transferred quickly to an electric furnace and set to 190C. The mixture was set to calcinate slowly up to 300°C, to remove all volatile products which result from the decomposition of the reactants without any solids escaping the crucible. The temperature of the furnace then increases to 350°C-400°C and the resulting molten glass was deposited into a stainless steel pre-form to be quenched. The obtained glass disks were 0.5 mm-1 mm in thickness and 20 cm-30 cm in diameter, with smooth glass surface characteristics optimal for the deposition of the AgCl solution.

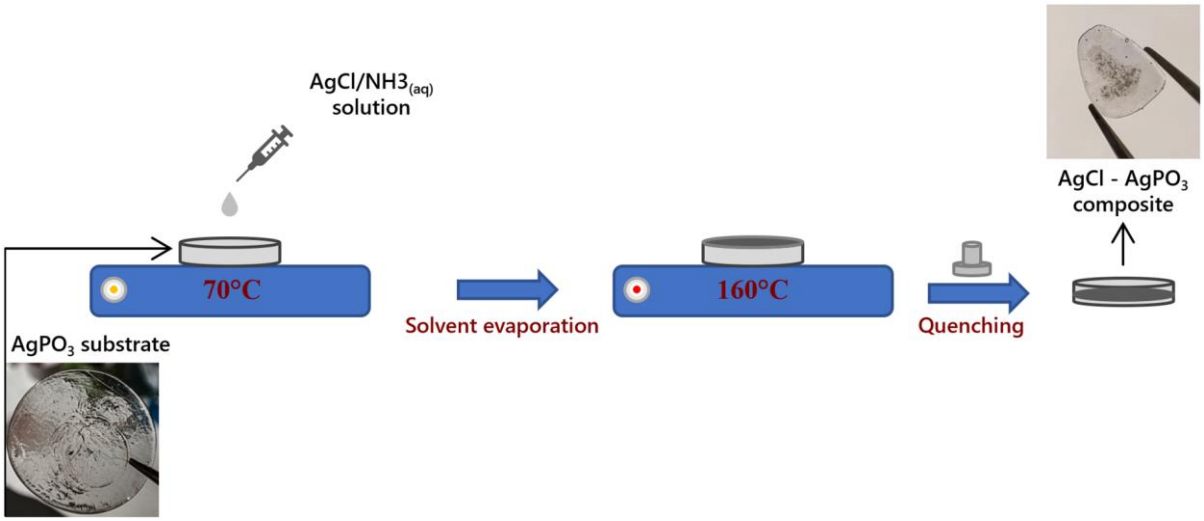

Figure 1: Schematic animation of the fabrication procedure.

Following the preparation of the glass substrate, we dissolved the AgCl solids in $NH_{3(aq)}$ (30% V/V aquatic), producing a solution with $8.3\overline{3}$% (w/v) AgCl-$NH_{3(aq)}$ weight of AgCl per volume of the $NH_{3(aq)}$ solution. Initially, we anticipated that the $NH_{3(aq)}$ solution would not produce any damage or residue due to a reaction with the surface of the substrate, which is also the reasoning behind the choice of an $NH_{3(aq)}$ solution instead of a strong electrolyte to dissolve the AgCl salt. Thus, with the evaporation of the dropped portion of salt solution onto the heated glass, it was expected that the solvent would have no effect to the substrate or final composite due to briefness of the procedure. This was refuted, with the observation of large yellow spotting on the surface of the glass after evaporation. It was confirmed that the $NH_{3(aq)}$ part of the solution had been reacting with the $AgPO_3$ substrate. To counter this, the AgCl-$NH_{3(aq)}$ solution was additionally diluted in aqua before deposition, with 0.5% and 0.75% w/v being the optimal final solutions (Table 1).

The $AgPO_3$ substrate split into equal area and thickness parts and placed into a silica wafer on the heating plate. A 3μL droplet of the AgCl-$NH_{3(aq)}$ solution is then spread on the surface of the substrate sample, and the temperature is set to calcinate slowly to 160°C to evaporate the solvent and uniformly release the residual AgCl compound, to be then quenched into the glass on a film form, due to the substrates close to Tg softness. After quenching, the wafer is removed from heat and the sample is left to cool and the photochromic composite is formed and stored into vacuum to avoid residual moisture on the surface. A schematic animation of the fabrication procedure is being presented in Figure 1.

2.2 Characterization

A UV lamp set to 254 nm has been used to irradiate the AgCl-$AgPO_3$ samples to their darkened phase, in durations of 20-60 seconds per sample. The irradiation conditions for each

sample are summarized in Table 1. All irradiations were performed on environment at normal incidence. After irradiation, each fabricated composite's optical absorption were measured in a PerkinElmer UV/Vis (Lambda 950) spectrometer over the wave-length range of 320-1200 nm. The surfaces of the composites have been examined field-emission scanning electron microscopy, while Raman spectroscopy was performed to explore any network modifications that the substrate may sustained due to the AgCl incorporation. Room temperature Raman spectra with a resolution of 1 cm^{-1} were collected at the backscattering geometry by employing a 532-nm laser line for excitation. In addition, the composite glasses were thoroughly examined by field-emission scanning electron microscopy (JEOL, JSM-7000F).

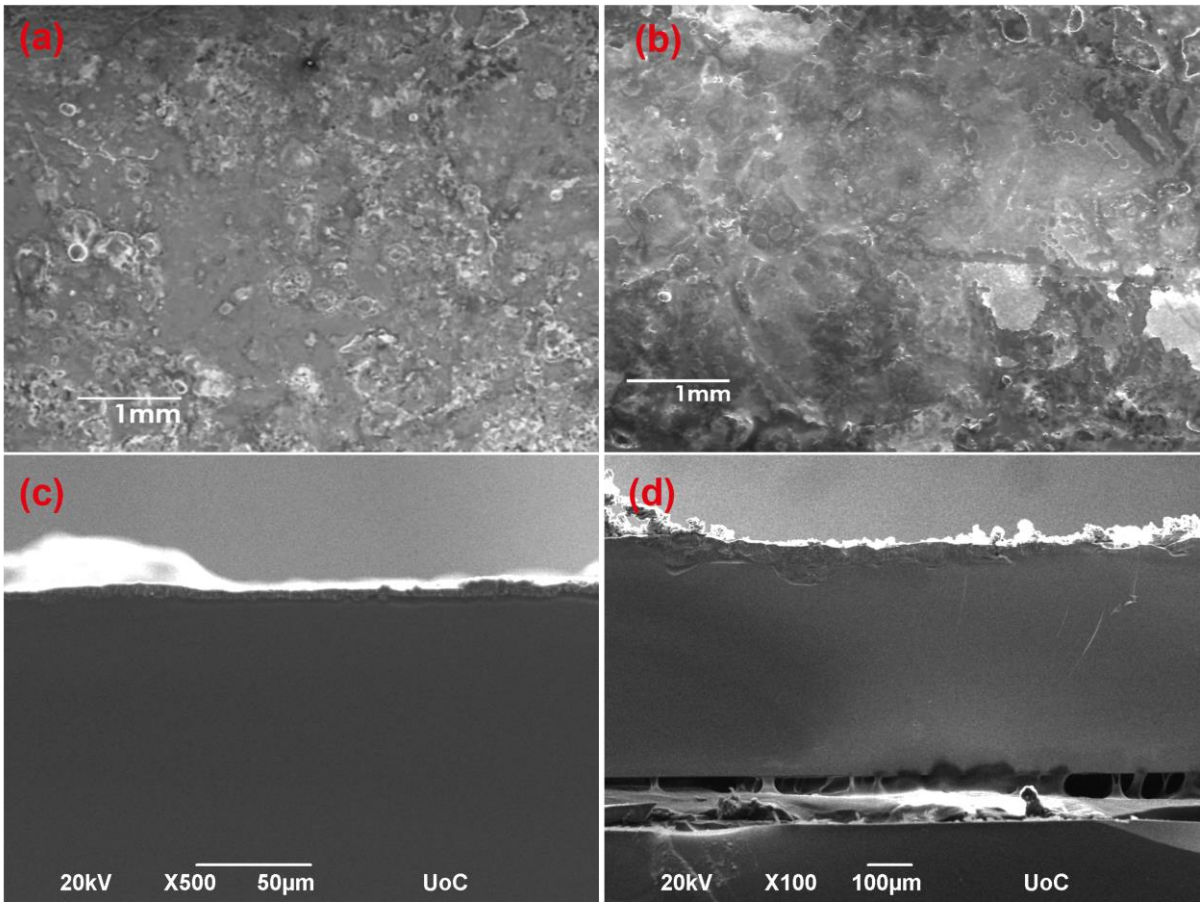

Figure 2: Scanning electron microscopy (SEM) images of the surface of sample A class AgCl-$AgPO_3$ composite (a) and the surface of sample B class composite (b). Cross-section image of sample A class composite (c) and sample B class composite (d).

3 Results and Discussion

3.1 AgCl-$AgPO_3$ composite glasses structural characterization

Figure 2 presents scanning electron microscopy (SEM) images of two samples prepared with each of the prepared solutions [0.5%-0.75% (w/v) AgCl-$NH_{3(aq)}$ (samples ’A’ and ’B’ respectively)] (see Table 1). Images of the surface of sample ‘A’ and ‘B’ can be seen in Figure 2a and Figure 2b, while cross-section images of sample ’A’ and ’B’ are presented in Figure 2c and Figure 2d respectively. Inspection of Figure 2a and Figure 2b reveals evidence of the vitrification of the AgCl on the $AgPO_3$ surface, although not uniformly without further surface treatment. Through the cross-sectional SEM-photographs in Figure 2c and 2d, it can be observed that the film has been submerged into the host glass in depths of up to 100μm. Comparison between sample A and B presents a significant distinction between the visible amount of AgCl residing both on the substrate’s surface and internally, an indicator that the encapsulated amount of AgCl depends on the concentration of the salt in the initial AgCl-$NH_{3(aq)}$ solution. This phenomenon is apparent in the SEM-photographs, where sample B (0.75%) shows significantly more complex crystalline structures on the surface layer of the substrate compared to the sample A counterpart, as well as during the synthesis procedure where the output composite, prepared with a richer AgCl solution, presents a more rough appearance on its surface.

Then, it was of great interest to examine whether the encapsulation of the AgCl, as well as any unintended reactivity between the $NH_{3(aq)}$ solvent and the $AgPO_3$, have induced any structural modifications of the –host phosphate glass network. The metaphosphate glass network generally consists of chains which are formed by the connection of phosphate tetrahedral units having bridging and non-bridging oxygen atoms. As seen in Figures 3b and 3d where the Raman spectra of the pristine $AgPO_3$ parts of the composite was measured, there is a distinct presence of the key bands of 1125 cm^{-1} and 686 cm-1 attributed at the symmetric

stretching vibration of terminal PO2- groups Vs(PO2-) and P-O-P Vs(P-O-P) respectively. Inspecting Figure 3a and 3b, Raman spectra of the surface of sample A and B, we can see an additional band at 1000 cm^{-1} and a slight alteration in the population of the $AgPO_3$ bands, which is indicative of a modification of the glass network. This can be attributed to the oversaturation of certain sections of the surface area of the composite by excess AgCl, in the form of crystals, as can be seen in Figure 2a and Figure 2b. It is plausible that the additional band originates from moisture developed in the surface of the glass after preparation, an effect visible if the composite is left to rest in humid environment for prolonged durations.

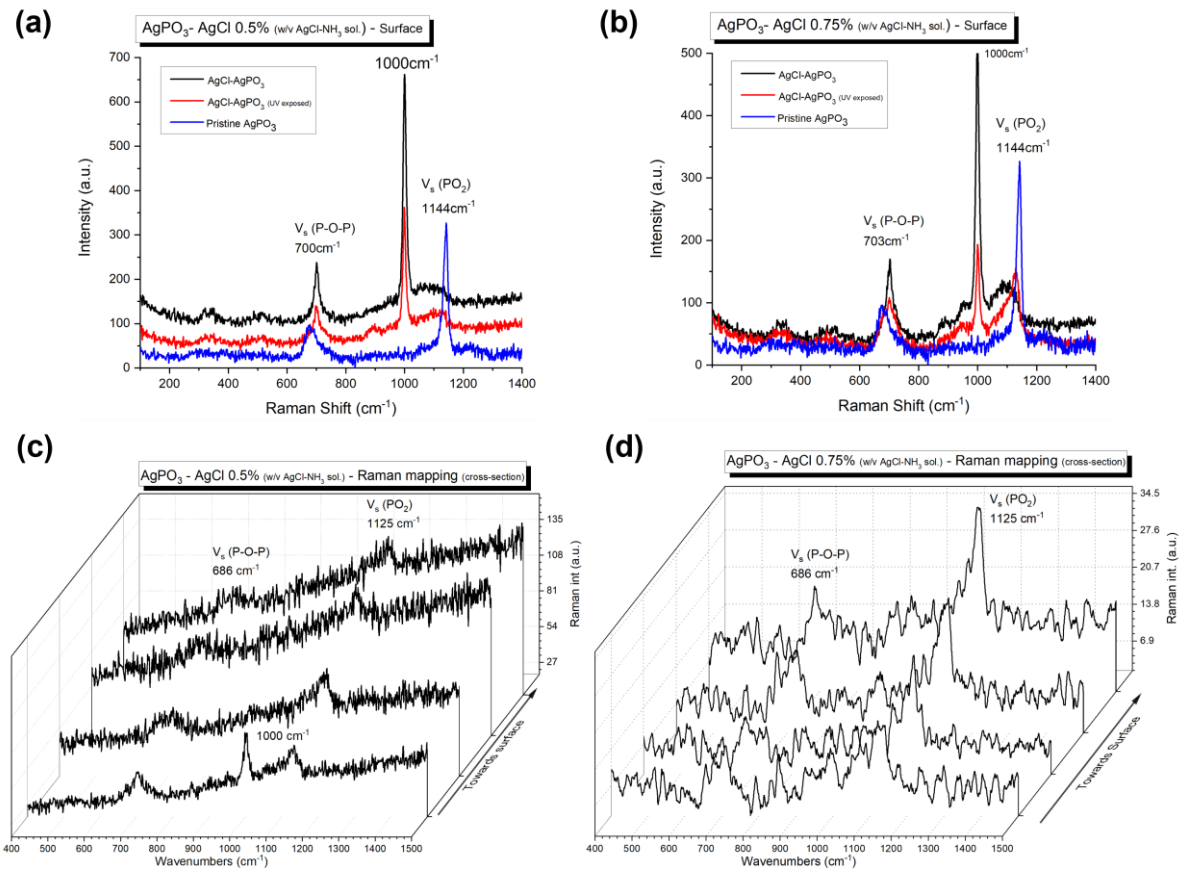

Figure 3: a Room-temperature Raman spectra at the surface of pristine, unexposed and UV exposed AgCl-$AgPO_3$ composite glass of sample A (a) and at the surface of sample B (b). Raman mapping spectra of the cross-section cut of sample A (c) and sample B (d).

As seen in Figures 3c and 3d where the Raman spectra of the cross-sectional parts of the composite was measured, only the aforementioned key bands are present. Thus, no major alterations present in the cross-sectional regions of the glass due to its almost pristine $AgPO_3$ surface, although as can be seen if Figure 3c, there as still signs of the 1000 cm^{-1} , further providing evidence of residual moisture.

Sample	$AgCl\text{-}NH_{3(aq)}$ %(w/v) / amount (μL)	Exposure - 254 nm (seconds)
A1	0.5 / 3	20
A2	0.5 / 3	40
A3	0.5 / 3	60
B1	0.75 / 3	20
B2	0.75 / 3	40
B3	0.75 / 3	60

Table 1: Summary of $AgCl\text{-}NH_3$ solution compositions and UV-exposure durations for $AgCl\text{-}AgPO_3$ composites with darkening and bleaching properties shown in Figures 5,6.

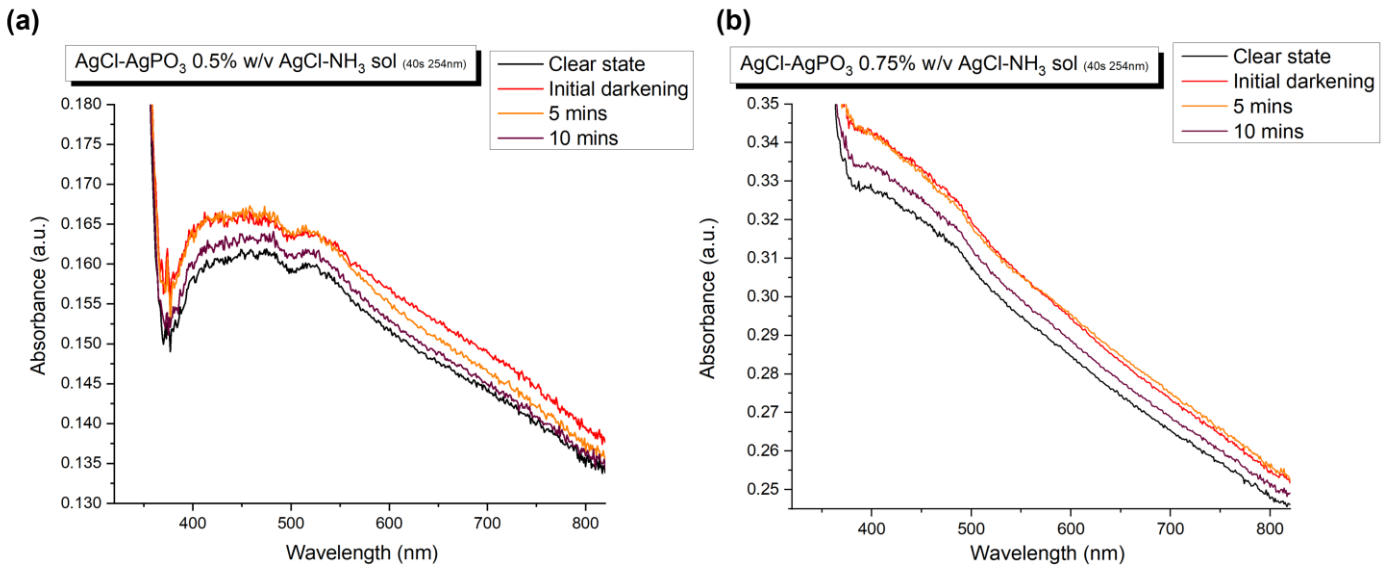

Figure 4: Optical absorbance spectra of the 40s UV-exposed sample A (a) and sample B (b).

3.2 AgCl-$AgPO_3$ composite glasses reversible photochromicity

Through the course of this research, we have studied a wide range of different factors, that can either greatly enhance or suppress, the photochromic properties of AgCl. It's switching mechanism is rather simple· when exposed under the activating UV light source, the silver ions separate from the halogens, reducing the composite's transparency and increasing its absorbance. When the light source is no longer applied, or a bleaching wavelength is present, the silver ions recombine with the chloride ions, increasing its transparency, reducing the absorptivity [17]. Therefore, it can be safely deduced that the resulting photochromicity of the composite is strongly dependent on the concentration of the photochromic component, it's ability to transition between the two states of variable transmissivity fluently, and the duration of it's exposure to the activating UV radiation.–

We have synthesized numerous amounts of AgCl-$AgPO_3$ glass composite samples, produced with AgCl-$NH_{3(aq)}$ solutions of with 0.1% to over 1% w/v AgCl as seen in Table 2, doses of 1μL to 15μL on the same host glass area, and measured the optical absorbance of composites exposed to 20s-60s of 254 nm UV radiation. In addition, we point out at this point that the photochromic switching ability of this composite is presented only in terms of its bare-bones characteristics, to solidify its prospective as a proof-of-concept for further development.

Figure 4 presents the optical absorbance measurements of both sample A and B whilst still unexposed to UV and remeasured in three distinctive moments after exposure. First post-exposure measurement were taken immediately after a 40s exposure period, and two consecutive measurements were taken after the initial, approximately 5 minutes and 10 minutes post-exposure. Figure 4a shows a smoother reverting transition for sample A, with steps of higher distinction , especially so on the 5 minute mark. Figure 4b presents sample B, where a sharp decline in absorbance in the 5 to 10 minutes mark can be seen. An interesting observation is that although sample B seemingly shows accelerating decrease in absorption throughout the

320-850 nm wavelength, both samples showed a resistance in bleaching on the first 5 minutes post-exposure, specifically in the 380-550 nm part of the spectra.

Avoiding the overflowing of the substrate with solution, almost exclusively provided with more uniform layers of AgCl film, due to the solution's apparent surface tension that spread the residual AgCl either in visually grainy spots or on the circumference of the glass. Sample A and B prepared with 3μL of 0.5% and 0.75%, have both presented an exceptional combination of photochromic properties, combining the beneficial attributes of composites produced in either boundary of the parametric procedure. Both samples have shown easily observable switching capabilities, with an almost immediate darkening of the glass after a few seconds of exposure, in combination to the apparent complete reverting to its original state in minutes. Remarkably enough, both samples A and B show the beneficial traits of each of their higher and lower AgCl concentration counterparts, in terms of darkening/bleaching time and visibility of the phenomenon, without being excluded from the consistency provided by the simplicity of the synthesis procedure.

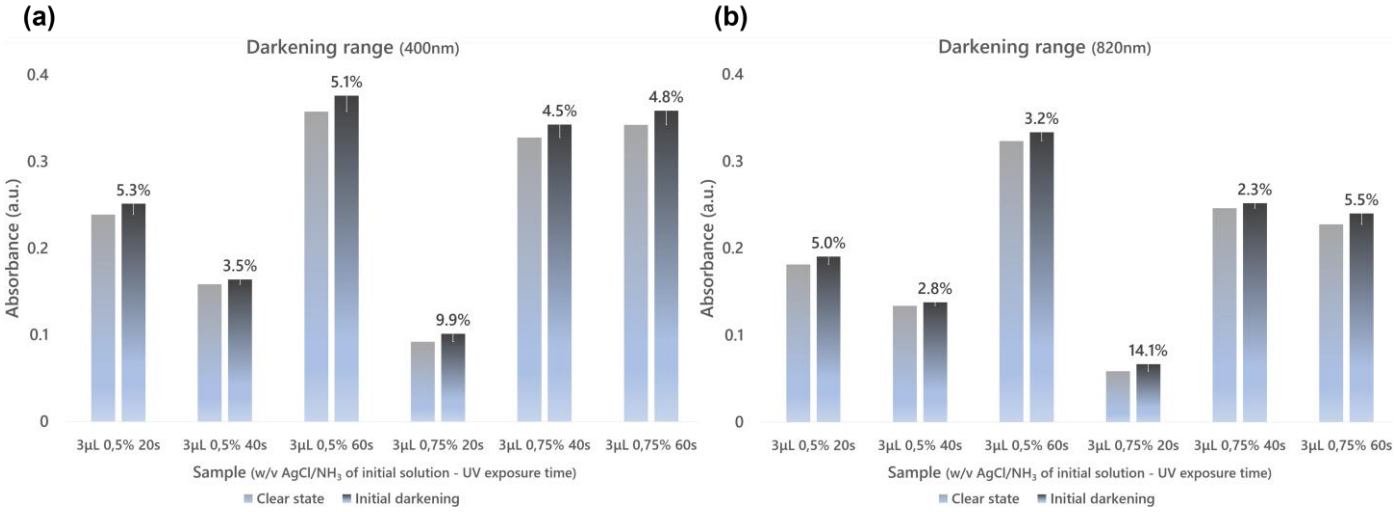

Figure 5: Darkening range bar graphs measuring absorbance at 400nm (a) and 820nm immediately post-exposure (b) for three types of sample A class and three types of sample B class exposed in different durations.

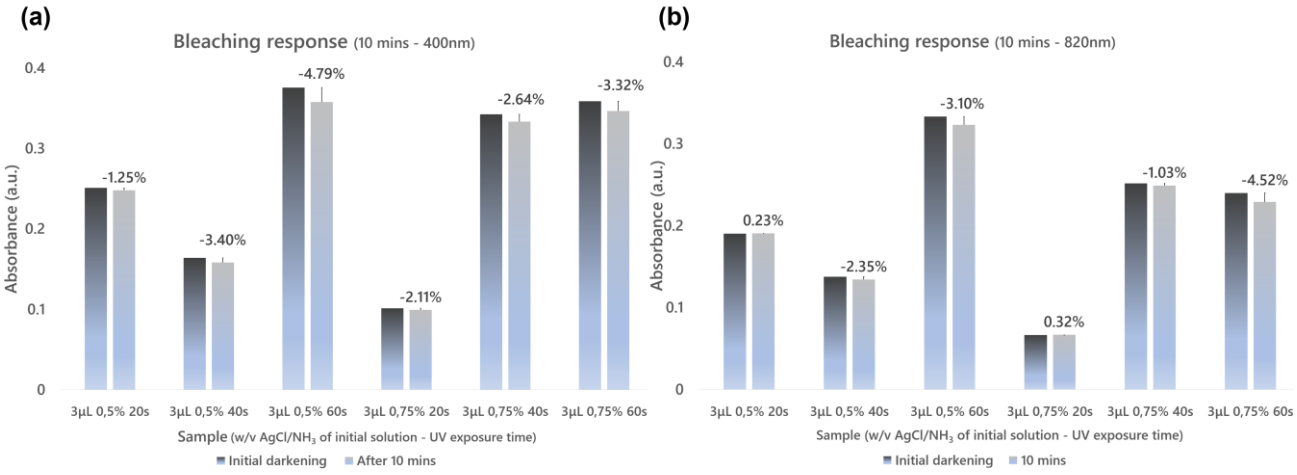

Figure 6: Bleaching response bar graphs measuring absorbance 10 minutes post-exposure at 400 nm (a) and 820nm (b) for three types of sample A class and three types of sample B class exposed in different durations.

We were able to produce and test at least six samples of the sample A class and six of the sample B class, with equivalent switching attributes between composites of the same group, albeit with differences in the outcome roughness of the surface due to the handheld quenching procedure, resulting in differences on the reflectivity and transmissivity of the composite glass.

Moreover, Figure 5 presents a bar graph for the percentile increase in absorption from the point of initial UV-exposure to the 10 minute mark, chosen to be referred to as darkening range, of six samples half of which were prepared in the specification of sample A and half were prepared in the specification of sample B. The three samples of each group were UV exposed in durations of 20s, 40s, and 60s and their optical absorbance was measured. In particular, Figure 5a shows the absorbance at 400 nm, whereas Figure 5b at 820 nm. The results show a coherent response of the samples to the irradiation, with specific cases from Figure 5a such as the 20s exposed sample A and B class composites increasing their 400nm absorbance 5.3% to 9.9% respectively, on 20 seconds of UV exposure. Similarly, as it can be seen in Figure 5b, 820nm absorbance has also seen an increase, most apparently so for the 20s exposed sample B class sample, showing an increase of 14.1%, in 20 seconds of irradiation. Inspection of Figure 5 suggests that the darkening response of the samples is not necessarily linearly proportional

to the duration of the exposure time on the first minute under UV, but also a function of the composite's initial absorbance. Differences in initial optical absorbance measured in samples of the same specification can also be attributed in the aforementioned variation in the surface roughness of each sample, affected by the quenching procedure and the uniform spread of the initial solution on the substrate. Additionally, even though most samples appear uniformly transparent to the naked eye, there are sections of the composite with higher and lower transparency. The afformentioned characteristic is also prominent in the cross-sectional images of Figure 2c and 2d, where the AgCl has evidently submerged in different depths throughout the surface of glass, resulting in areas of lower transparency. To limit such effects, low temperature surface treatments such as surface smoothing are suggested.

In addition, Figure 6 presents a bar graph for the percentile decrease in absorbance from the point of initial UV-exposure to the 10 minute mark, chosen to be referred to as bleaching response, i.e. indicative of the reversing photochromic response. These results firmly connect with the darkening range data, to provide evidence that both samples A and B have a fluency in reverting back to mostly revert back to their original clear state, within the 10 minute threshold, regardless of the span of their darkening. Samples that were exposed in durations of 40s and 60s, feature higher bleaching response, in the same 10 minute time-frame than their 20s-exposed counterparts, especially when investigating the 400 nm part of the spectra as Figure 6a suggests. Specimen such as the 60s-exposed sample A class composite, although it did not have the highest overall darkening range, it completely reverted back to its original state, in less than 5 minutes in the dark. Interestingly, even though the darkening range of the samples did not follow a linear upwards trend in absorption after exposure with the increase in exposure time as can be seen in Figure 5, the opposite can be seen in both cases of Figure 6. The bleaching response of all the samples of either sample A class or sample B class, follow an upward trend in the amount of decrease of the absorption, following the increase in UV-

exposure time. In a noteworthy case, the 20s-exposed sample B class sample had the largest absorbance increase, at both 400 nm and 820 nm wavelengths, and the smallest absorbance decrease during the bleaching phase.

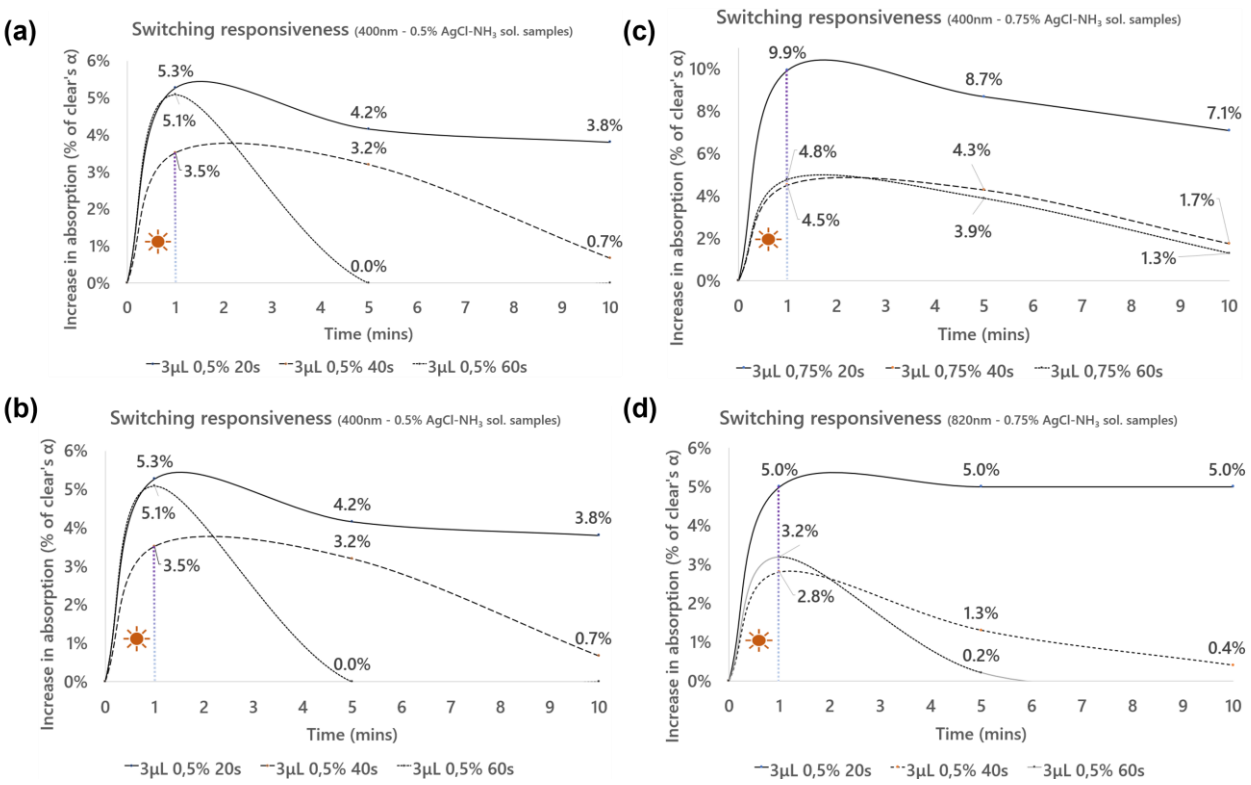

Figure 7: Switching responsiveness measured in percentile difference of the optical absorbance relative to the pre-exposured from pre-exposure to 10 minutes post exposure. (a) Samples of class A at 400 nm, (b) samples of class A at 820nm, (c) samples of class B at 400 nm, (d) samples of class B at 820 nm.

Sample	$AgCl\text{-}NH_{3(aq)}$ %(w/v)	Remarks
1	0.1	Great transparency , limited switching response
2	0.3	Great transparency, moderate darkening response, good bleaching response
A	0.5	Great transparency, great darkening/bleaching response
B	0.75	Great transparency, great darkening/bleaching response
5	1	Subpar transparency, high sensitivity, high darkening response, very slow bleaching
6	1.5	Almost non-transparent, very high sensitivity, unable to revert

Table 2: Summary of $AgCl\text{-}AgPO_3$ samples produced with variable compositions of $AgCl\text{-}NH_{3(aq)}$ solutions.

For a more thorough demonstration of the data on darkening range and bleaching response of the samples, Figure 7 depicts, the complete switching progression of all tested samples, from pre-exposure to 10 minutes post-exposure, chosen to be referred to as switching responsiveness. Namely, Figure 7 shows the percentile difference in absorbance relative to the initial, pre-exposure absorbance value of each sample. In addition to Figure 5 and Figure 6, Figure 7 also takes into consideration the absorbance measurements made in the 5 minute checkpoint. Figure 7a and Figure 7b present the switching responsiveness of the three sample A class composites UV-exposed at three different exposure times, and measured at 400nm and 820nm respectively. Figure 7c and Figure 7d follow the same pattern for the three sample B class samples, at the same wavelengths. Similarly to Figure 5,6 , trends of a sharper decrease in absorbance can be seen for the samples irradiated for longer periods of time, on both types of samples and wavelengths. These graphs emphasize on the composite's sensitivity to increase its absorbance noticeably even after very short periods of UV-exposure, whilst also showing its ability to almost completely revert back to its original state in a brief manner.

Undoubtedly, the most significant indicator of improvement in the tuning phase of the synthesis procedure was the apparent and easily reversible photochromic response of the samples when exposed under UV. Composites prepared with solutions with either inadequate portions of the solution or with solutions of very low AgCl concentration, required prolonged periods of UV exposure to show a limited amount of coloration, if any. Whilst composites prepared with over-saturating portions of AgCl-$NH_{3(aq)}$ solution, or solutions of very high AgCl concentration, presented immediate coloring response to the radiation, but with poor ability (or complete inability) to revert back to its bleached state. Both sample A and B show ability to switch briefly between states, an attribute granted by the balanced specification of their composition, in-between limited and excessive sensitivity concentrations.

4 Conclusions

In conclusion, we herein demonstrate a simple and low temperature post-glass quenching method for the incorporation of AgCl photochromic films within a transparent phosphate glass matrix. The developed method enables substantially lower-temperature encapsulation of the photochromic compound withing the glass matrix, and consecutively providing a lower energy alternative for photochromic composite glasses, when compared to composites based on silica glass. Additionally, we studied the composite's behavior when exposed to brief durations UV-exposure, to demonstrate its potential to applications where a milder but substantially quicker photochromic response is required. Based on this, the described non-toxic, self-resorbable vitrification procedure using the metaphosphate glass matrix, is proven to be a suitable method to produce fatigueless, high sensitivity, highly responsive AgCl photochromic glass composites.

5 ACKNOWLEDGMENTS

We would like to thank A. Manousaki (IESL, FORTH) for her technical assistance with SEM studies, and Dr. A. S. Sarkar (IESL, FORTH) for his help with Raman spectroscopy. This work is partially supported by TheSmartMat project, "Laser-assisted development of composite thermochromic materials for energy smart and safe buildings", ΕΣΠΑ2014-2020, RIS3Crete, G.A. KPHP1-0032623.

6 REFERENCES

[1] B. Kumar Babu, S. Ghosh, S. Chakrabortty, Recent developments in smart window engineering: from antibacterial activity to self-cleaning behavior, Energy Saving Coating Materials. (2020) 227–263. https://doi.org/10.1016/B978-0-12-822103-7.00010-8.

[2] M. Hočevar, U. Opara Krašovec, A photochromic single glass pane, Solar Energy Materials and Solar Cells. 186 (2018) 111–114. https://doi.org/10.1016/J.SOLMAT.2018.06.035.

[3] H. Miyazaki, T. Ishigaki, T. Ota, Photochromic Smart Windows Employing WO3-Based Composite Films, Journal of Materials Science Research. 6 (2017) 62. https://doi.org/10.5539/JMSR.V6N4P62.

[4] P. Wang, S. Yan, Y. Du, Y. Tao, D. Chen, Fabrication and photochromic properties of Al2O3–CaO binary glasses, Journal of Non-Crystalline Solids. 576 (2022) 121257.

https://doi.org/10.1016/J.JNONCRYSOL.2021.121257.
[5] H. Zhang, Z. Chen, C. Zhu, C. Wei, An innovative and smart road construction material: thermochromic asphalt binder, New Materials in Civil Engineering. (2020) 691–716. https://doi.org/10.1016/B978-0-12-818961-0.00022-3.
[6] M. Soltani, A.B. Kaye, Properties and Applications of Thermochromic Vanadium Dioxide Smart Coatings, Intelligent Coatings for Corrosion Control. (2015) 461–490. https://doi.org/10.1016/B978-0-12-411467-8.00013-1.
[7] C.G. Granqvist, Fenestration for reducing building cooling needs: an introduction to spectral selectivity, thermochromics, and electrochromics, Eco-Efficient Materials for Mitigating Building Cooling Needs: Design, Properties and Applications. (2015) 441–471. https://doi.org/10.1016/B978-1-78242-380-5.00016-9.
[8] G. Yang, Y.M. Zhang, Y. Cai, B. Yang, C. Gu, S.X.A. Zhang, Advances in nanomaterials for electrochromic devices, Chemical Society Reviews. 49 (2020) 8687–8720. https://doi.org/10.1039/D0CS00317D.
[9] S. Morsümbül, E.P. Akçakoca Kumbasar, Photochromic textile materials, IOP Conference Series: Materials Science and Engineering. 459 (2018) 012053. https://doi.org/10.1088/1757-899X/459/1/012053.
[10] D.T. Christiansen, A.L. Tomlinson, J.R. Reynolds, New Design Paradigm for Color Control in Anodically Coloring Electrochromic Molecules, Journal of the American Chemical Society. 141 (2019) 3859–3862. https://doi.org/10.1021/JACS.9B01507/SUPPL_FILE/JA9B01507_SI_001.PDF.
[11] V.A. Barachevsky, 2D materials for smart energochromic sunscreen devices, 2D Nanomaterials for Energy Applications: Graphene and Beyond. (2020) 173–208. https://doi.org/10.1016/B978-0-12-816723-6.00007-1.
[12] J. Zhang, Q. Zou, H. Tian, Photochromic Materials: More Than Meets The Eye, Advanced Materials. 25 (2013) 378–399. https://doi.org/10.1002/ADMA.201201521.
[13] H. Miyazaki, H. Shimoguchi, H. Suzuki, T. Ota, Synthesis of photochromic AgCl-urethane resin composite films, Advances in Materials Science and Engineering. 2012 (2012). https://doi.org/10.1155/2012/784202.
[14] R. Talebi, Investigating multicolour photochromic behaviour of AgCl and AgI thin films loaded with silver nanoparticles, Physical Chemistry Chemical Physics. 20 (2018) 5734–5743. https://doi.org/10.1039/C7CP07923K.
[15] Photochromic lenses: Transitions and other light-adaptive lenses, (n.d.). https://www.allaboutvision.com/lenses/photochromic.htm (accessed January 21, 2022).
[16] Silver Chloride (AgCl) Optical Material, (n.d.). https://www.crystran.co.uk/optical-materials/silver-chloride-agcl (accessed January 21, 2022).
[17] H. Miyazaki, H. Shimoguchi, H. Nakayama, H. Suzuki, T. Ota, Effects of excess Cu addition on photochromic properties of AgCl-urethane resin composite films, Advances in Materials Science and Engineering. 2013 (2013). https://doi.org/10.1155/2013/854928.
[18] A.S. Sarkar, I. Konidakis, I. Demeridou, E. Serpetzoglou, G. Kioseoglou, E. Stratakis, Robust B-exciton emission at room temperature in few-layers of MoS2:Ag nanoheterojunctions embedded into a glass matrix, Scientific Reports 2020 10:1. 10 (2020) 1–10. https://doi.org/10.1038/s41598-020-72899-3.
[19] I. Konidakis, E. Skoulas, A. Papadopoulos, E. Serpetzoglou, E. Margariti, E. Stratakis, Erasable and rewritable laser-induced gratings on silver phosphate glass, Applied Physics A: Materials Science and Processing. 124 (2018). https://doi.org/10.1007/S00339-018-2267-0.
[20] I. Konidakis, K. Brintakis, A. Kostopoulou, I. Demeridou, P. Kavatzikidou, E. Stratakis, Highly luminescent and ultrastable cesium lead bromide perovskite patterns generated in phosphate glass matrices, Nanoscale. 12 (2020) 13697–13707. https://doi.org/10.1039/D0NR03254A.

[21] D. Palles, I. Konidakis, C.P.E. Varsamis, E.I. Kamitsos, Vibrational spectroscopic and bond valence study of structure and bonding in Al 2 O 3 -containing AgI–AgPO 3 glasses, RSC Advances. 6 (2016) 16697–16710. https://doi.org/10.1039/C6RA00162A.
[22] H. Nakazumi, S. Matsumoto, K. Isagawa, Photochromic behavior of spiropyrans in glass thin films formed by the sol-gel method, Advanced Materials ’93. (1994) 323–326. https://doi.org/10.1016/B978-1-4832-8380-7.50080-8.
[23] I. Konidakis, A. Karagiannaki, E. Stratakis, Advanced composite glasses with metallic, perovskite, and two-dimensional nanocrystals for optoelectronic and photonic applications, Nanoscale. (2022). https://doi.org/10.1039/D1NR07711B.